Simulation of the Movement of Beads by the DEM with Respect to the Wet Grinding Process

Dariusz Gudin, Roman Turczyn, Hiroshi Mio, Junya Kano, and Fumio Saito
Institute of Multidisciplinary Research for Advanced Materials, Tohoku University, Sendai 980-8577, Japan

DOI 10.1002/aic.10956
Published online August 30, 2006 in Wiley InterScience (www.interscience.wiley.com).

This work has shown a method for simulating the motion of beads in a bead mill based on the discrete element method (DEM) under wet grinding of a gibbsite powder, in correlation with the experimental work. The beads' motion was simulated under a wet condition and compared with the real motion observed and recorded by a video camera. At the base of the simulation the specific impact energy of beads was calculated. In the experiment, the gibbsite powder, suspended in water at 5.0 wt %, was subjected to grinding by the bead mill at different operating conditions. Particle-size distribution of the product was measured and the grinding rate constant of the sample was determined as a change in the mean particle size of the ground product with time. Then, the specific impact energy was correlated with the grinding rate constant determined experimentally. It was found that good correlation between the two was achieved and by the proposed method the particle size reduction of the sample can be predicted. © 2006 American Institute of Chemical Engineers *AIChE J,* 52: 3421–3426, 2006
Keywords: simulation, grinding, gibbsite, beads motion, impact energy

Introduction

Milling is an important operation in reduction of the size of particles and has been carried out in many fields of science and industry. Such operation can be done by using several types of mills, and recently much attention has focused on the *bead mill* because of its capability of producing fine particles. The main reason that a bead mill facilitates the production of such fine particles is attributed to the fine beads, ranging in size from 20 to 50 μm. In addition, the bead mill can disperse fine aggregates into well-dispersed fine particles.

There have been several types of bead mill developed over the course of the last decade, one of which is a bead mill[1] that consists of a horizontally positioned grinding chamber with an agitator that is attached with a slurry tank connecting with a circulation system. The chamber is filled with grinding beads and a slurry. The grinding performance for the feed material in a mill is dependent on the motion of the beads, which can be controlled by many operating conditions such as the rotational speed, the shape of the agitator, the diameter of the beads, the filling ratio, and the sample charge. When the media (beads) motion in a mill is simulated three-dimensionally, the impact energy of the media can be calculated.[2-5] Therefore, the simulation of media motion would be a key factor to understand the grinding performance of a solid powder sample, and this would yield useful information on optimization of the milling condition as well as scaling-up the mill device.

One of the simulation routes would be a method based on the *discrete element method* (DEM),[6] which has been applied to simulation of media motion in a mill under dry grinding operation.[2-5,7] With respect to the wet milling, however, because of the difficulty in description of the model in the DEM under wet condition, little information has been reported. In our attempt to simulate the media (balls) motion in a tumbling mill under wet condition,[8] we concluded that the grinding rate constant of gibbsite can be correlated with the specific impact energy of the balls simulated. This implies that the grinding performance of the sample ground under wet condition in a tumbling mill can be predicted by the simulation of the balls' motion under any operating conditions. In the present work, we have extended it into a method for simulating the media motion in a bead

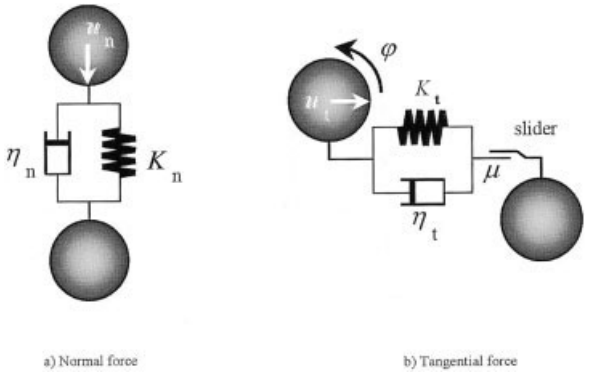

Figure 1. Model of interactive forces between two media balls.[2]

mill to predict the grinding performance of a gibbsite powder under wet condition.

Simulation

The simulation method presented herein enables us to give the interactive forces between two beads and their relative impact velocities and positions at each time step, leading to the trajectory of each bead during the milling.[6] The shapes of the grinding chamber and the agitator are constructed with a series of planes. In the simulation the agitator is a full cylinder with nine pins, without openings. The determined time step keeps the overlap between the beads during collision within a reasonable range below 1%, although a small percentage of collisions can exceed this value. The contact on collision between two bodies is expressed by the simulation model shown in Figure 1, which consists of a spring, a dashpot, and a slider. The interactive force F_i at the collision is calculated from Eq. 1, where K and η are the spring and damping coefficients, respectively, and u is the relative displacement.

$$F_i = Ku + \eta \frac{du}{dt} \tag{1}$$

The motion of beads in wet condition is influenced by the slurry, so that the drag force F_D and the buoyancy have to be considered. The F_D is calculated by Eq. 2, where C_d is the drag coefficient, A is the projection area of a bead, ρ_s is the density of slurry, and u_r is the relative velocity between the bead and slurry:

$$F_D = C_d A \rho_s \frac{u_r^2}{2} \tag{2}$$

The C_d is calculated by Eqs. 3 and 4,[9] depending on the value of the Reynolds number Re, and Eq. 5, where d_B is the bead diameter and α is viscosity of the slurry:

$$10^{-4} < \mathrm{Re} < 1 \qquad C_d = \frac{24}{\mathrm{Re}} \tag{3}$$

Table 1. Constants Used in the Calculation

Density of beads (g/cm^3)	6.0	
Young's modulus (GPa)	21.0	
Poisson's ratio	0.30	
Time step (s)	1.1×10^{-6}	
Slurry density (kg/m^3)	998.0	1029.0
Slurry dynamic viscosity (mPa · s)	0.94	1.1

$$1 < \mathrm{Re} < 10^4 \qquad C_d = \frac{24}{\mathrm{Re}} + \frac{3}{\sqrt{\mathrm{Re}}} + 0.34 \tag{4}$$

$$\mathrm{Re} = \frac{d_B |u_r| \rho_s}{\alpha} \tag{5}$$

To reduce the computational time, the flow rate of the slurry is modeled by Eq. 6,[10] on the assumption that the slurry is an incompressible and Newtonian fluid and the flow is determined from the rotational direction of the agitator. In the equation, r is the radius and v_θ is the slurry velocity:

$$\frac{d}{dr}\left[\frac{1}{r}\frac{d}{dr}(rv_\theta)\right] = 0 \tag{6}$$

The buoyant force F_B for beads is calculated by Eq. 7, where V_B is the volume of the bead:

$$F_B = V_B \rho_s \tag{7}$$

The motion of a bead is calculated from Newton's Second Law, described by Eq. 8, where a is the acceleration of the bead, m is the mass of the bead, g is the gravitational acceleration, and F is the resultant force:

$$a = \frac{F}{m} + g \tag{8}$$

The motion of beads in the slurry is influenced by their surface roughness. Therefore, the coefficient of friction μ and the slurry viscosity should be considered in the simulation model.

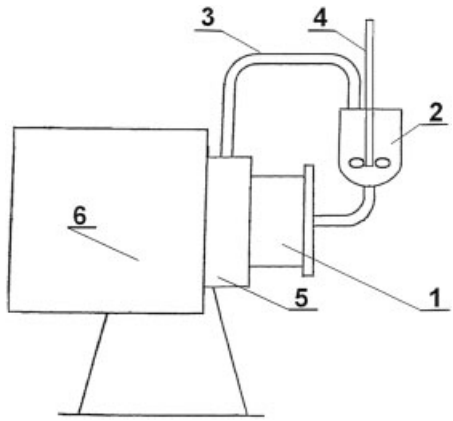

Figure 2. Bead mill.

1: Grinding chamber; 2: slurry tank; 3: recirculation system; 4: mixer; 5: recirculation pump; 6: drive.

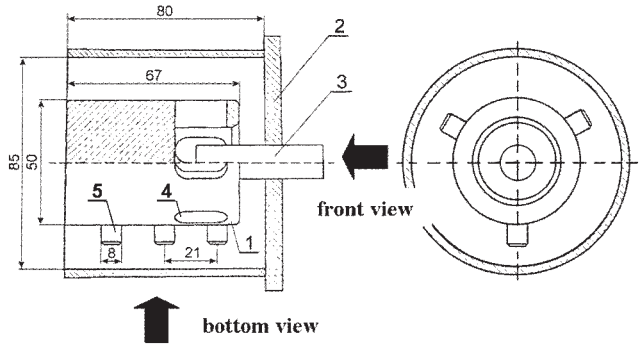

Figure 3. Grinding chamber.

1: Agitator; 2: front lid; 3: connector pipe; 4: opening (6 pcs.); 5: pin (9 pcs.).

The most suitable value of μ can be estimated by comparing the motion simulated with that observed in the experiment. In researched conditions the values of the coefficients of friction between beads and between a bead and the wall are $\mu_i = 0.2$ and $\mu_w = 0.25$, respectively. To accelerate the calculation with results kept at the proper level, the Young's modulus of beads smaller than the real value is taken. Parameters used in the calculation are shown in Table 1.

The specific impact energy of beads E_w can be calculated from the relative velocity v_j on collision between two beads or a bead against the mill wall by Eq. 9, where W is the mass of the sample charged in the mill and t_s is the simulation time:

$$E_w = \frac{\sum \frac{1}{2} m v_j^2}{W t_s} \tag{9}$$

Experimental

The mill used in the experiment is a MiniZeta bead mill (Netzsch GmbH, Selb, Germany); the schematic diagram of the experimental equipment is shown in Figure 2. The grinding chamber and the agitator are made of stainless steel. To visualize the beads' motion, the front lid of the chamber or whole chamber was replaced with transparent parts, without connection with the circulation system. The dimensions of the chamber are 85 mm diameter and 80 mm length. Free volume of the chamber is 350 cm^3. Between the front lid and the agitator there is a gap 13 mm wide. The agitator is a partly hollow cylinder 50 mm in diameter, with six elongated openings and nine cylindrical pins, as shown in Figure 3. The rotational speed of the agitator can be fixed in the range from 600 to 3300 rpm. Five sets of yttrium-stabilized zirconia (YSZ) beads 0.5, 1.0, 1.5, 2.0, and 3.0 mm in diameter were used. The volume of each set of the beads was 200 cm^3. The movement of the beads near transparent parts of the chamber was observed from the front and the bottom views in dry and wet conditions at 600, 800, 1000, 1200, 1800, and 2400 rpm in rotational speed of the agitator and recorded with a digital video camera. A sample used in the experimental work was gibbsite [$Al(OH)_3$, Sumitomo Chemical Co., Tokyo, Japan]. The 50% initial particle size D_0 was 56.8 μm, determined by using a particle size analyzer (Microtrac S3000, Nikkiso, Tokyo, Japan). The sample was dispersed in water at a solid concentration of 5.0 wt %. Conditions of the experiments are shown in Table 2.

Table 2. Experimental Conditions

Grinding chamber volume (cm^3)	350					
Rotational speed (rpm)	600	800	1000	1200	1800	2400
Volume of beads (cm^3)	200					
Diameter of beads (mm)	0.5	1.0	1.5	2.0	3.0	
Slurry concentration (%)	0.0			5.0		

Results and Discussion

Motion of beads in the mill

To confirm that the DEM model is applicable to the computer simulation of the beads' motion in the bead mill, the simulated results were compared with the movement of the beads observed in the mill without the presence of slurry. According to the preliminary experiment, the 2-mm beads show a cataracting motion of the beads in the chamber under the dry condition at 600 rpm. At 1200 to 1800 rpm, they show rotational motion. With respect to the 1-mm beads, they show rotational motion at 1800 rpm only, whereas the 0.5-mm beads show the cataracting motion. Figure 4 shows real and simulated motions of the 2-mm beads in dry condition at 600 and 1200 rpm. It can be seen that the motion of the beads in the simulation is similar to that observed experimentally. This implies that the present method for simulating the beads' motion could be suitable for predicting the beads' motion in the bead mill under dry condition.

In the wet grinding process, the motion of beads is similar to that observed in the dry condition, although for the same rotational speed of the agitator, the beads move much faster.

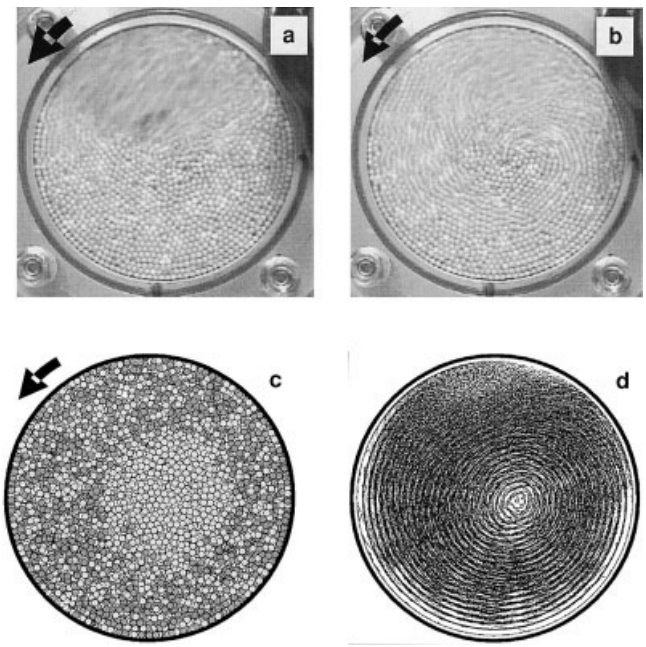

Figure 4. Motion of beads in dry condition.

Yttrium-stabilized zirconia (YSZ): $d_B = 2$ mm. (a) cataracting motion ($N = 600$ rpm); (b) rotational motion ($N = 1200$ rpm); (c) simulation ($N = 1200$ rpm); (d) beads' trajectories ($N = 1200$ rpm).

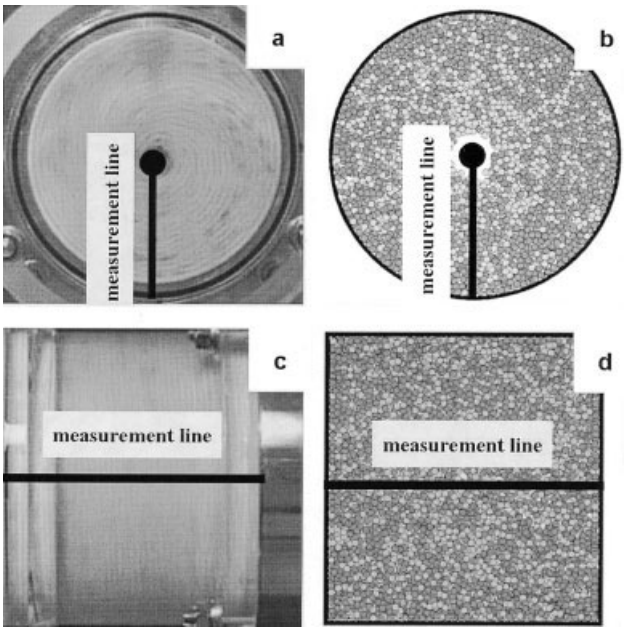

Figure 5. Motion of beads in wet condition.

YSZ: d_B = 2 mm, C = 0%, N = 1200 rpm. (a) and (c) real motion; (b) and (d) simulation.

Because of the higher value of the centrifugal force of the beads, a free space in the center of the grinding chamber can be observed. Figure 5 shows real and simulated motions of 2-mm beads in the bead mill under the wet condition. For all cases, at the lower part of the chamber there is a zone where the movement of the beads is ordered. Measurement of the velocity of beads at the line marked in Figure 5 can help us to assess simulation results. The central space 50 mm in diameter and 13 mm wide between the agitator and the front lid was not compared because of difficulty with observation of the beads' motion close to the center of the grinding chamber. This space is roughly 7% of the free volume of the chamber and during the milling operation is partly filled with a connector pipe, as shown in Figure 3.

Figures 6 and 7 show experimental and simulation velocities of the beads observed from the front and bottom views for the slurry concentration C = 5% at agitator speeds of 600 and 1200 rpm. The circular flow of slurry is calculated by Eq. 6 and close to the lids of the chamber a linear reduction of slurry velocity is introduced. The movement of the beads near the front lid is slower than that inside of the chamber. This may be a result of the friction of the beads against the lid and the presence of a gap between the agitator and the lid. As expected, the higher rotational speed of the agitator produces the higher velocity of the beads. The simulated results are satisfactorily consistent with experimental ones.

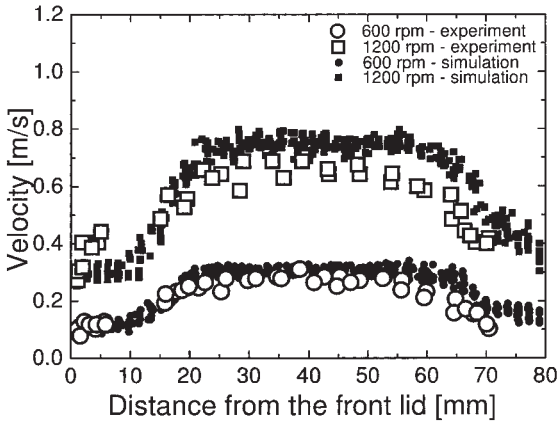

Figure 7. Velocity of the beads in wet conditions observed from the bottom view.

YSZ: d_B = 2 mm, C = 0%, μ_i = 0.2, μ_w = 0.25.

Size distribution of the product and grinding rate constant

Figure 8 shows the particle distribution curves of the sample ground for various times by using the 2-mm YSZ beads under C = 5%, N = 1200 rpm. Extension of the grinding operation causes a decrease of particle size, although quick size reduction occurs in the early stage of the

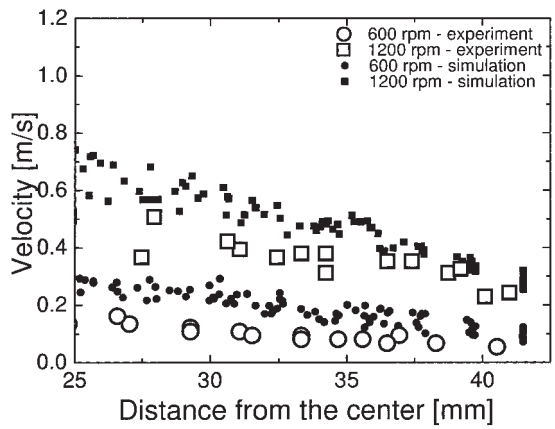

Figure 6. Velocity of the beads in wet conditions observed from the front view.

YSZ: d_B = 2 mm, C = 5%, μ_i = 0.2, μ_w = 0.25.

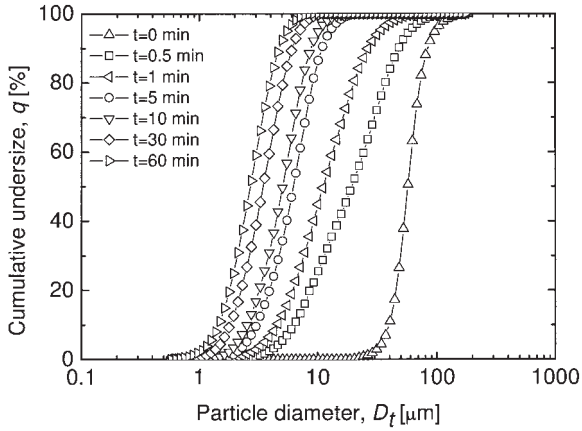

Figure 8. Particle-size distribution curves of the sample ground for various periods of time.

YSZ: d_B = 2 mm, C = 5%, N = 1200 rpm.

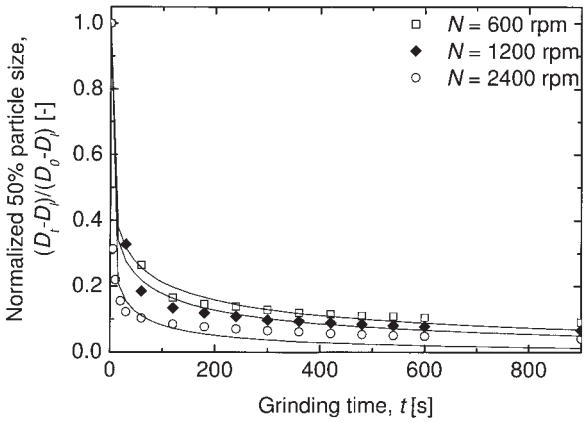

Figure 9. Normalized 50% particle size for various values of the rotational speed of the agitator *N*.

YSZ: d_B = 2 mm, C = 5%.

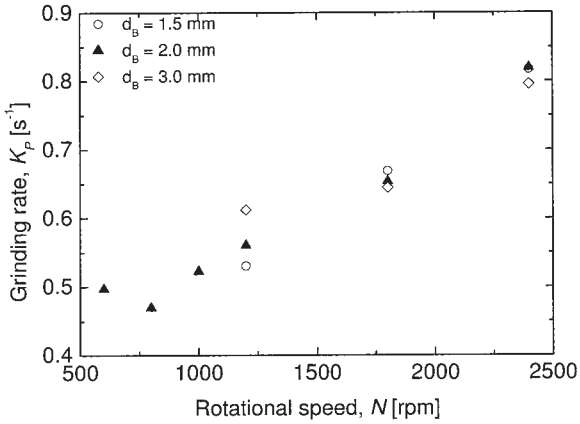

Figure 11. Grinding rate constant of the sample as a function of the rotational speed *N*.

YSZ: C = 5%.

operation. Figures 9 and 10 show the normalized 50% particle size $(D_t - D_l)/(D_0 - D_l)$ as a function of the grinding time t, for various values in the rotational speed of the agitator and the diameter of the beads. The plotted values are experimental data and the lines are calculated from Eq. 10. Increasing the rotational speed and decreasing the diameter of the grinding media enable us to improve the grinding performance.

Figure 11 shows the grinding rate constant K_P defined by Eq. 10 as a function of the rotational speed. In the equation D_t is the 50% particle size at an arbitrary grinding time, D_l is the 50% particle size of the finest sample among all experiments, and D_0 is the 50% particle size at the initial stage.

$$\frac{D_t - D_l}{D_0 - D_l} = \exp(-K_P t^{0.25}) \tag{10}$$

Figure 12 shows the specific impact energy per unit time E_w, calculated from all collisions between beads and between a bead and the agitator or the wall of the chamber, as a function of the rotational speed. This relationship is similar in trend to that between K_P and N. An increase in the rotational speed of the agitator causes higher specific impact energy, resulting in the higher value of the grinding rate constant.

Figure 13 represents the relationship between the grinding rate constant of the sample and the calculated specific impact energy for various values in the rotational speed of the agitator and diameter of beads. The correlation between the two confirms that the specific impact energy obtained from the simulation of beads' motion in the mill would be useful for predicting the grinding rate constant and the particle size of the sample in the bead mill under wet condition. Figure 14 shows the relation between 50% particle size and time of grinding. The experimental data are consistent with prediction.

Conclusion

The method for simulating the motion of the beads in the bead mill wet condition was introduced in this article. In the experiment, the gibbsite powder, suspended in water, was subjected to grinding by the bead mill under different conditions. Particle size distribution of the product was measured and the grinding rate constant of the sample was determined as a change in the mean

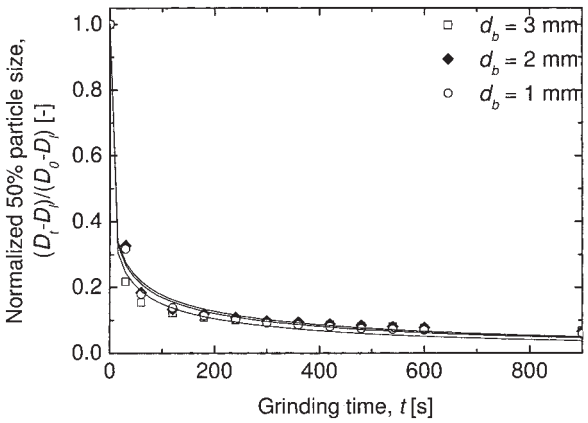

Figure 10. Normalized 50% particle size for different beads sizes.

YSZ: C = 5%, N = 1200 rpm.

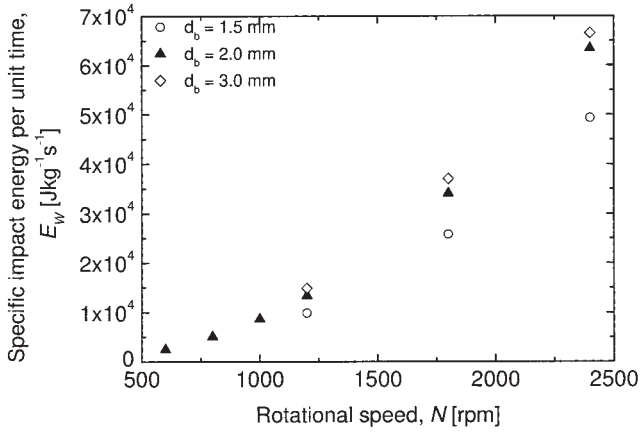

Figure 12. Specific impact energy calculated as a function of the rotational speed.

YSZ: C = 5%.

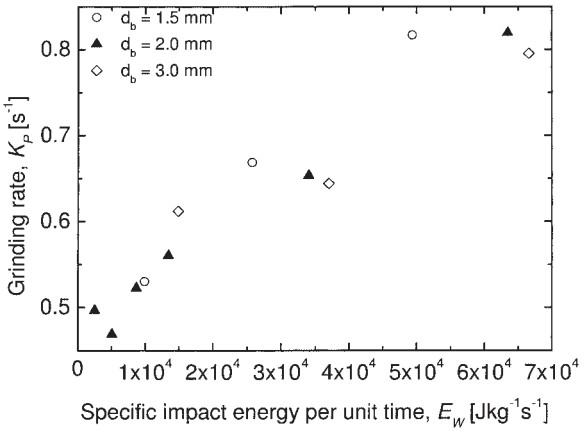

Figure 13. Correlation between the grinding rate constant K_P and the specific impact energy E_w for different operating conditions.

particle size of the ground product with time. The obtained results allowed us to formulate the following conclusions:

(1) The motion of beads in a wet bead mill can be simulated by the proposed method based on the DEM model. The proper coefficient of friction and slurry flow model play important roles in the simulation of beads' motion under wet condition.

(2) The specific impact energy of the beads obtained from the simulation is correlated with the grinding rate constant of the sample obtained experimentally. This would yield useful information on the milling operation, leading to optimization of wet grinding conditions.

Notation

A = projection area of grinding media, m^2
a = acceleration, $m^2 \cdot s^{-1}$
C = concentration of suspension, wt %
C_d = drag coefficient
D_0 = 50% particle size at initial stage, μm
D_l = 50% particle size of the finest sample among all experiments, μm
D_t = 50% particle size at arbitrary grinding time, μm
d_B = bead diameter, m
E_w = specific impact energy of beads per unit time, $J \cdot kg^{-1} \cdot s^{-1}$
F = resultant force, N
F_B = buoyant force, N
F_D = drag force, N
F_i = interactive force, N
g = gravitational acceleration, $m \cdot s^{-2}$
K = spring coefficient
K_P = grinding rate constant, s^{-1}
m = mass of grinding media, kg
N = rotational speed of the agitator, rpm
r = radius, m
Re = Reynolds number
t = grinding time, s
t_s = simulation time, s
u = displacement, m
u_r = relative velocity between the bead and suspension, $m \cdot s^{-1}$
V_B = volume of the bead, m^3
v_j = relative velocity of beads on collision, $m \cdot s^{-1}$
v_θ = slurry velocity, m/s
W = mass of sample, kg

Greek letters

α = viscosity of slurry, mPa·s
η = damping coefficient
μ_i = coefficient of friction between beads
μ_w = coefficient of friction between a bead and the wall
ρ_s = density of suspension, $kg \cdot m^{-3}$

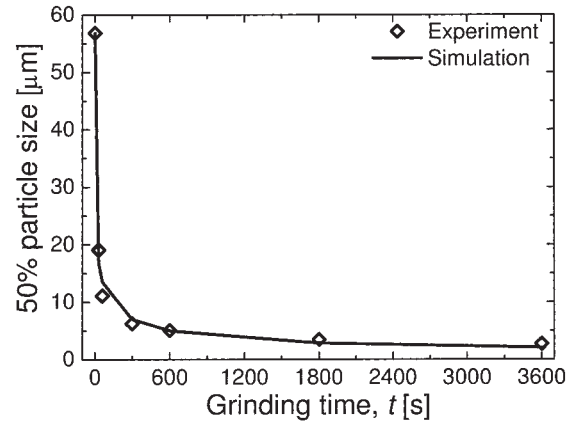

Figure 14. Simulated 50% particle size of the sample ground for various periods of time.

YSZ: d_B = 2 mm, C = 5%, N = 1200 rpm.

Literature Cited

1. Kwade A. Wet comminution in stirred media mills—Research and its practical application. *Powder Technol*. 1999;105:14-20.
2. Kano J, Chujo N, Saito F. A method for simulating the three-dimensional motion of balls under the presence of a powder sample in a tumbling ball mill. *Adv Powder Technol*. 1997;8:39-51.
3. Kano J, Miyazaki M, Saito F. Ball mill simulation and powder characteristics of ground talc in various types of mill. *Adv Powder Technol*. 2000;11:333-342.
4. Kano J, Mio H, Saito F, Miyazaki M. Correlation of grinding rate of gibbsite with impact energy in tumbling mill with mono-size balls. *Miner Eng*. 2001;14:1213-1223.
5. Mio H, Kano J, Saito F, Kaneko K. Effects of rotational direction and rotation-to-revolution speed ratio in planetary ball milling. *Mater Sci Eng*. 2002;A332:75-80.
6. Cundall PA, Strack ODL. A discrete numerical model for granual assemblies. *Geotechnique*. 1979;29:47-.
7. Mishra BK, Rajamani RK. The discrete element method for the simulation of ball mills. *Appl Math Model.* 1992;16:598-604.
8. Mori H, Mio H, Kano J, Saito F. Ball mill simulation in wet grinding using a tumbling mill and its correlation to grinding rate. *Powder Technol.* 2004;143/144:230-239.
9. Fair GM, Geyer JC. *Water Supply and Waste-Water Disposal*. New York: Wiley; 1954.
10. Kou S. *Transport Phenomena and Materials Processing*. New York: Wiley; 1996:63.

Manuscript received Apr. 27, 2005, revision received Mar. 16, 2006, and final revision received Jun. 28, 2006.